High speed engine gas thermometry by Fourier-domain mode-locked laser absorption spectroscopy

Laura A. Kranendonk[1,2], Xinliang An[1], Andrew W. Caswell[1], Randy E. Herold[1], Scott T. Sanders[1*], Robert Huber[3, 4], James G. Fujimoto[3], Yasuhiro Okura[5], and Yasuhiro Urata[5]**

[1]*Engine Research Center, University of Wisconsin - Madison, 1500 Engineering Dr, Madison, WI 53706 – USA*
[2]*Current Address: Oak Ridge National Laboratory, 2360 Cherahala Blvd., Knoxville, TN 37931 - USA*
[3]*Department of Electrical Engineering and Computer Science and Research Laboratory of Electronics, Massachusetts Institute of Technology,77 Massachusetts Ave, Cambridge, MA 02139 - USA*
[4]*Lehrstuhl für BioMolekulare Optik, Fakultät für Physik, Ludwig-Maximilians-Universität München, Oettingenstr. 67, 80538 Munich – Germany*
[5]*Department 1, Technology Research Division 2, Honda R&D Co., LTD., Tochiigi R&D Center, 4630 Shimotakanezawa Haga-machi Haga-gun Tochigi, 321-3393 – Japan*
**Corresponding author: ssanders@engr.wisc.edu;*
***Corresponding author: Robert.Huber@Physik.Uni-Muenchen.DE*

Abstract: We present a novel method for low noise, high-speed, real-time spectroscopy to monitor molecular absorption spectra. The system is based on a rapidly swept, narrowband CW Fourier-domain mode-locked (FDML) laser source for spectral encoding in time and an optically time-multiplexed split-pulse data acquisition system for improved noise performance and sensitivity. An acquisition speed of ~100 kHz, a spectral resolution better than 0.1 nm over a wavelength range of ~1335-1373 nm and a relative noise level of ~5 mOD (~1% minimum detectable base-e absorbance) are achieved. The system is applied for crank-angle-resolved gas thermometry by H_2O absorption spectroscopy in an engine motoring at 600 and 900 rpm with a precision of ~1%. Influences of various noise sources such as laser phase and intensity noise, trigger and synchronization jitter in the electronic detection system, and the accuracy of available H_2O absorption databases are discussed.

OCIS codes: (120.6200) Spectrometers and spectroscopic instrumentation; (140.3600) Lasers, tunable; (170.6280) Spectroscopy, fluorescence and luminescence; (300.1030) Absorption; (300.6260) Spectroscopy, diode lasers; (300.6340) Spectroscopy, infrared.

References and links

1. S. T. Sanders, D. W. Mattison, L. Ma, J. B. Jeffries, and R. K. Hanson, "Wavelength-agile diode-laser sensing strategies for monitoring gas properties in optically harsh flows: application in cesium-seeded pulse detonation engine," Opt. Express, **10**, (2002) 505-514.
2. M. A. Oehlschlaeger, D. F. Davidson, and R. K. Hanson, "Investigation of the reaction of toluene with molecular oxygen in shock-heated gases," Combust. Flame **147**, 195-208 (2006).
3. F. C. De Lucia, Jr., R. S. Harmon, K. L. McNesby, K. L. Winkel Jr., R. J. and A. W. Miziolek, "Laser-induced breakdown spectroscopy analysis of energetic materials," Appl. Opt. **42**, 6148-6152 (2003).
4. A. Suslov, B. K. Sarma, J. B. Ketterson, F. Balakirev, A. Migliori, and A. Lacerda, "Ultrasonic Instrumentation for Measurements in High Magnetic Fields. II. Pulsed Magnetic Fields" in *11th International Conference on Ion Sources, 2005*, "Ultrasonic Instrumentation for Measurements in High Magnetic Fields. II. Pulsed Magnetic Fields" (AIP, Caen, France, 2006), pp. 35105-35111.
5. L. A. Kranendonk, R. Huber, J. G. Fujimoto, and S. T. Sanders, "Wavelength-agile H_2O absorption spectrometer for thermometry of general combustion gases," Proc. Combust. Inst. **31**, 783-790 (2007).
6. L. A. Kranendonk, J. W. Walewski, T. Kim, and S. T. Sanders, "Wavelength-agile sensor applied for HCCI engine measurements," Proc. Combust. Inst. **30,** 1619-1627 (2005).
7. A. W. Caswell, S. T. Sanders, and M. J. Chiaverini, "Swept-Wavelength Laser Absorption Tomography for Imaging Rocket Plume Gas Properties" in *41st AIAA/ASME/SAE/ASEE Joint Propulsion Conference and*

#87089 - $15.00 USD Received 31 Aug 2007; revised 19 Oct 2007; accepted 23 Oct 2007; published 31 Oct 2007

Exhibit, "Swept-Wavelength Laser Absorption Tomography for Imaging Rocket Plume Gas Properties", (2005).
8. L. A. Kranendonk and S. T. Sanders, "Optical design in beam steering environments with emphasis on laser transmission measurements," Appl. Opt, **44**, (2005) 6762-6772.
9. R. A. Palmer, J. L. Chao, R. M. Dittmar, V. G. Gregoriou, and S. E. Plunkett, "Investigation of Time-Dependent Phenomena by use of Step-Scan FT-IR" in *Symposium on Advanced Infrared Spectroscopy (AIRS)*, "Investigation of Time-Dependent Phenomena by use of Step-Scan FT-IR," Tokyo, Japan, (1993) 1297-1310.
10. R. Huber, M. Wojtkowski, and J. G. Fujimoto, "Fourier Domain Mode Locking (FDML): A new laser operating regime and application for optical coherence tomography," Opt. Express **14**, 3225-37 (2006).
11. C. L. Hagen and S. T. Sanders, "Investigation of Multi-species (H_2O_2 and H_2O) Sensing and Thermometry in an HCCI Engine by Wavelength-Agile Absorption Spectroscopy," Meas. Sci. Technol. **18**, 1992-1998 (2006).
12. J. A. Filipa, J. W. Walewski, and S. T. Sanders, University of Wisconsin, 1500 Engineering Dr., Madison, WI 53706, are preparing a manuscript to be called "Optical beating in time-resolved spectroscopy. Part II: Strategies for spectroscopic sensing in the presence of optical beating".
13. J. W. Walewski, J. A. Filipa, and S. T. Sanders, University of Wisconsin, 1500 Engineering Dr., Madison, WI 53706, are preparing a manuscript to be called "Optical beating of polychromatic light and its impact ontime-resolved spectroscopy. Part I: Theory".
14. J. W. Goodman, "Some problems involving high-order coherence," in *Statistical Optics* (John Wiley & Sons, Inc., 1985), pp. 237-250.
15. M. J. Beran and Jr. G. Parrent, *Theory of Partial Coherence*, (Society of Photo-Optical Instrumentation Engineers, Palos Verdes Estates, 1974).
16. S. T. Sanders, "Online thermal beating noise calculator," http://chyp.erc.wisc.edu/tools/thermallight.html.
17. R. Huber, M. Wojtkowski, K. Taira, J. G. Fujimoto, K. Hsu, "Amplified, frequency swept lasers for frequency domain reflectometry and OCT imaging: design and scaling principles," Opt. Express **13**, 3513-3528 (2006).
18. R. Huber, D. C. Adler, J. G. Fujimoto, "Buffered Fourier domain mode locking: unidirectional swept laser sources for optical coherence tomography imaging at 370,000 lines/s," Opt. Lett. **31**, 2975- 2977 (2006).
19. R. E. Herold, D. E. Foster, J. B. Ghandhi, R. J. Iverson, J. A. Eng, and P. M. Najt, "Fuel unmixedness effects in a gasoline homogeneous charge compression ignition engine," Int. J. Engine Res. **8**, 241-257 (2007).
20. L. A. Kranendonk, A. W. Caswell, and S. T. Sanders, "Robust method for calculating temperature, pressure and absorber mole fraction from broadband spectra," Appl. Opt. **46**, 4117-4124 (2007).
21. R. J. Barber, J. Tennyson, G. J. Harris, and R. N. Tolchenov, "A high-accuracy computed water line list," Monthly Notices of the Royal Astronomical Society **368**, 1087-1094 (2006).

1. Introduction

Transient spectroscopic sensing can be useful in studies of events such as detonations [1], shock waves [2], explosions [3], pulsed magnetic fields [4], and various propulsion devices [5-7]. In most of these applications, one generally wishes to acquire spectra at rates of 10 kHz – 1 MHz in real time. There are at least two reasons that such high speeds may be required. First, properties of interest can change quickly in these transient environments and high speeds are required to resolve these changes. Second, even if properties of interest are relatively slowly varying, high-speed spectroscopy may be desired for immunity to noise; high-speed approaches can place the molecular information at frequencies above the characteristic noise frequencies (e.g., beam steering noise [8]).

Sampling techniques, such as step-scan Fourier transform spectroscopy [9], pump-probe spectroscopy, time gated and other stroboscopic techniques can also be used to resolve dynamic processes. However, these techniques are limited to highly repetitive processes or processes that can be triggered in time. In the case of optical triggering and detection, high radiation intensities are required in order to measure the non-linear absorption/emission properties. Even for processes meeting these prerequisites, sampling techniques are not always desirable because of increased acquisition time, sensitivity to changing environmental conditions or sample degradation. Comparisons between this and other optical thermometry techniques can be found in the literature [5, 6]. The work presented in this paper relates to thermometry in a piston engine. Although the engine process is roughly repeatable, one important research interest relates to cycle-by-cycle variations in gas temperature. Sampling techniques are essentially unable to provide such information, and this is one reason we have chosen to pursue real-time spectroscopy to study this process.

#87089 - $15.00 USD Received 31 Aug 2007; revised 19 Oct 2007; accepted 23 Oct 2007; published 31 Oct 2007

High speed spectroscopy using rapidly swept laser sources has proven to be a powerful tool for fast real-time spectroscopy. A laser with a narrow linewidth is repeatedly tuned over the spectral range of interest and the time-dependent transmission through the sample is recorded with a fast photodetector. When the time dependence of the laser wavelength is known, the recorded transient signal can be converted into an absorption/transmission spectrum of the sample. In such laser spectroscopy setups the system performance greatly depends on the properties of the laser source. For the described application, sweep speeds of 4nm/μs over a 40 nm range at an instantaneous linewidth of ~0.1 nm are desired.

The technique of Fourier domain mode locking (FDML) has been demonstrated to enable the design of narrowband swept laser sources with high sweep repetition rates and narrow instantaneous linewidth and low intensity noise [10]. In this study we describe an FDML laser especially designed for the application of monitoring combustion processes in piston engines. The laser is integrated into a novel setup using time-multiplexed, split pulse data-acquisition detection for improved noise performance. The time-dependent transmission is recorded and reduced to absorption spectra. We demonstrate the application of this system as an optical temperature sensor to monitor the gas temperature in a piston engine with high speed and high precision (better than 1% with crank-angle resolution). In this engine, gas conditions can in general vary from 300 K to 2200 K and from 0.7 bar to 35 bar, although in the measurements presented here, a smaller range of 300 – 800 K and 2 – 18 bar is spanned. The system must generally provide a temporal resolution of 1 crank angle degree (CAD), referenced to the piston motion. One CAD corresponds to 278 μs and 185 μs at the 600 rpm and 900 rpm speeds presented here and up to 56 μs at the fastest engine speed of 3000 rpm expected for such sensor applications.

2. Fundamental considerations

2.1 Suitable spectral range and resolution for gas temperature measurements

The described system is designed to measure time-resolved absorption in the region of 1335-1373 nm. The 1335-1373 nm range was carefully chosen as follows. Beginning by considering all possible options for thermometry by absorption spectroscopy, the wavelength range was narrowed to the telecom range to take advantage of readily available fiber and laser components. Available components offset some of the difficulty in building high-performance, swept-wavelength laser sources. Second, H_2O was chosen as the target molecule because it is the strongest absorber in this wavelength range in most combustion systems; furthermore, it can be easily seeded into flows when insufficient amounts are present. Next, within the above constraints, wavelength ranges of 1335-1373 nm (encompassing most of the R-branch of the $\nu_1+\nu_3$ band of H_2O) and 1385-1480 nm (encompassing most of the P-branch of the $\nu_1+\nu_3$ band of H_2O) were selected as two candidate ranges offering maximum temperature sensitivity over the expected conditions (300-800 K, 2-15 bar, and H_2O mole fraction ~ 3%). By monitoring a full rotational branch, one monitors all of the available temperature information from the spectra (all available lower-state energies). The 1335-1373 nm range was selected because it is the narrower of the two spectral ranges; at fixed performance, lasers sweeping over narrower ranges are easier to construct. Furthermore, it is known that a weak absorption due to H_2O_2 centered near 1420 nm can potentially interfere with H_2O in the 1385-1480 nm range [11]. The FDML laser operates at a spectral resolution of 0.1 nm or better. This resolution is sufficient to reveal the primary absorption features in the 1335-1373 nm range (which includes the majority of the R-branch of the $\nu_1+\nu_3$ band of H_2O, as well as contributions from other bands such as $2\nu_1$ and $2\nu_3$) at adequate signal-to-noise ratio. Because the laser sweeps through 38 nm with 0.1 nm resolution or better, each spectrum contains at least 380 spectral resolution elements. The laser is operated at 50% duty cycle, so that it is only on for 5 μs during each 10 μs interval to which a temperature value is ultimately assigned. Thus the laser sweeps through at least 380 spectral resolution elements in 5 μs, corresponding to a rate of at least 76 M elements/s. However, the laser wavelength sweeps as a sinusoidal function of time, so that the peak data

#87089 - $15.00 USD Received 31 Aug 2007; revised 19 Oct 2007; accepted 23 Oct 2007; published 31 Oct 2007

rate is at least 115 M elements/s. The oscilloscope samples at 100 MS/s, resulting in somewhat under-sampled data. This under-sampling ultimately contributes to the noise in the present temperature data and will be overcome in future tests by using a 400 MS/s oscilloscope.

2.2 Required noise performance of spectroscopy setup

Careful management of noise is generally important in high-speed spectroscopic systems. For example, we must use a laser source of sufficient power in order to limit shot noise. In the present experiments, the laser power transmitted through the engine and incident on the detector is ~ 1 mW. This power means approximately 68 M photons are incident upon the detector for every data point recorded every 10 ns by the oscilloscope, corresponding to a shot noise level of 0.012%. This noise level is about 10x smaller than other noise sources present in the experiment and therefore is considered acceptable.

Many recent high-speed spectroscopy experiments in the Engine Research Center have revealed a noise we have termed 'thermal beating noise' [12], also known as 'polychromatic beating noise' or 'optical beating noise'. This noise can exist whenever polychromatic radiation is incident upon the photoreceiver; the multiple frequencies can interfere or beat with each other in a chaotic fashion [13]. The noise is present, for example, when thermal emission (as from an incandescent lamp) is detected. However, the light source doesn't need to be truly thermal (black body radiator), only a dominantly non-coherent emission character is required. Amplified spontaneous emission sources also exhibit this noise. The relative noise level is generally highest when the spectral width of the source is narrow and the analog detection bandwidth is high. For the remainder of this paper, we refer to this noise simply as 'beating noise'. The reader interested in learning more about beating noise is referred to [14] and [15]. Note that fully coherent light sources like broadband femtosecond lasers with their fixed phase relation between individual modes do not exhibit this type of noise.

The FDML laser used in this work is similar to one that has been described previously [10], with one key difference: for this work, the tunable filter drive frequency was purposely detuned from the exact synchronization frequency with the cavity roundtrip time in order to improve linewidth. The drive frequency of the optical bandpass filter and the optical roundtrip frequency were detuned by about 3 Hz. This mode of operation was chosen in order to provide a stable linewidth, a smooth, continuous sweep operation and a high sweep to sweep stability over the complete spectral range (see section 3.1). However, in this slightly detuned mode, the FDML laser exhibits increased intensity noise relative to exactly synchronized operation. This increased noise is attributed to beating.

For a quantitative analysis of beating noise, the output of the FDML source will be modeled as the output of a 2 W CW thermal broadband source spanning 1335-1373 nm and post-filtered by a narrow spectral bandpass sweeping the same range. In reality, such a post-filtered source would not be economical owing to the 2 W power requirement in a single mode fiber; furthermore, 2 W easily exceeds the damage threshold of typical narrowband fiber-based filters. We consider the hypothetical source here only for the purposes of discussing beating noise. A photoreceiver viewing the output from the hypothetical source receives a 0.1-nm-wide spectral slice of 'white' light at any given instant. The different wavelengths within this slice beat with each other to create modulation in the observed intensity output; this beating appears as noise. As with many other noise sources, this type of noise becomes larger as the response time (or integration time) of the photoreceiver becomes shorter. Unlike most other noise sources, the amplitude of this noise increases as the bandwidth of the observed spectral slice is reduced. In the present experiment, the combination of high spectral resolution (0.1 nm ~ 1.6×10^{10} Hz) and short response time (~ 10 ns) yield a relative beating noise level of ~ 8% RMS [16]. This noise has another peculiar feature: it is essentially insensitive to the optical power levels. Therefore, this 8% noise level cannot be reduced by increasing the laser power. For example, a 4 W CW thermal broadband source would result in equivalent relative beating noise. However, the noise could be

#87089 - $15.00 USD Received 31 Aug 2007; revised 19 Oct 2007; accepted 23 Oct 2007; published 31 Oct 2007

eliminated altogether by replacing the thermal CW source in the above example with a broadband femtosecond laser source.

3. Experimental setup and system performance

3.1 FDML laser source

A Fourier Domain Mode Locked (FDML) laser functions as narrowband instantaneous bandwidth, cw light source which is rapidly swept in wavelength. FDML lasers have been introduced for high speed optical coherence tomography biomedical imaging in the 1300 nm wavelength region [10]. In FDML lasers, a tunable bandpass filter is driven synchronously with the optical roundtrip time of the light in a laser cavity. Light with a given wavelength passes through the filter, propagates through the cavity and arrives back at the filter at exactly the time when the filter is again tuned to the same spectral position. FDML produces a quasi-stationary operation regime for the laser and enables wavelength tuning of a laser without constraints in tuning speed caused by the build up dynamics in the cavity which are present in conventional wavelength swept lasers [17].

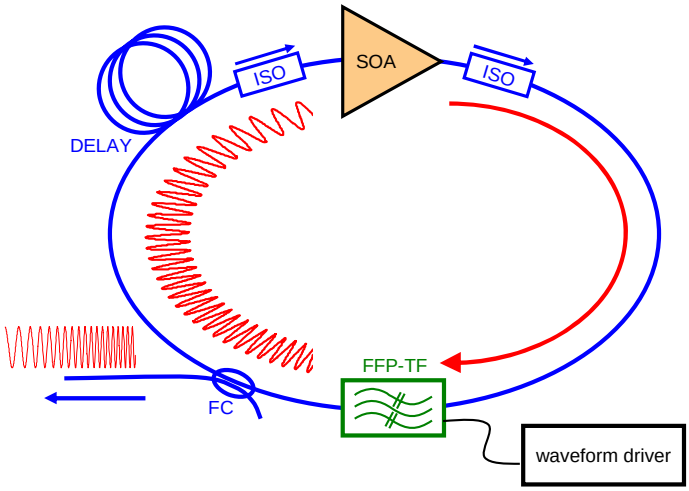

Fig. 1. Schematic of FDML laser. A semiconductor optical amplifier (SOA) acts as gain medium, two isolators (ISO) ensure unidirectional lasing, a fiber Fabry Perot tunable filter (FFP-TF) which is driven by a sinusoidal electronic waveform provides active wavelength selection, a fiber coupler (FC) extracts light from the cavity, and a 2 km spool of single mode fiber (DELAY) optically stores the swept waveform and enables synchronization to the filter tuning period.

Figure 1 shows a schematic of the laser used in experiments. The FDML laser is implemented as a fiber ring laser using a semiconductor optical amplifier (SOA; Inphenix, Inc.) as the gain medium, a fiber Fabry Perot tunable filter (FFP-TF; Micron Optics, Inc.) as an optical bandpass filter for active wavelength selection and a 2 km spool of standard single mode fiber (SMF 28e Corning) to increase the cavity length. The tunable filter was driven sinusoidally at 98.8545 kHz, about 3 Hz detuned from the resonance with the optical roundtrip time. 30% of the energy is extracted from the cavity by a fused fiber coupler placed after the FFP-TF for reduced ASE background noise. The SOA was modulated with a square wave, such that it was switched off during 50% of the time, resulting in 50% duty cycle and a sequence of unidirectional sweeps. Thus, each sweep covers a time window of about 5 μs followed by a gap of 5 μs. The operation is similar to the one in buffered FDML operation [18], however, in the case presented here the remaining time gap is not filled with a copy of

#87089 - $15.00 USD Received 31 Aug 2007; revised 19 Oct 2007; accepted 23 Oct 2007; published 31 Oct 2007

the original sweep but is rather used for the detection of a reference signal. The concept is described in detail in the following section 3.2.

In order to detect smallest absorption changes in spectroscopic applications, a highly stable intensity output is required. The intensity noise performance of the laser was investigated using a high speed analog-to-digital converter. Figure 2 is a thumbnail for the .avi movie associated with this article. The movie shows the transient intensity versus time for different drive frequencies of the laser. The intensity traces shown in Fig. 2 (.avi movie) were measured with a high time resolution of ~120 ps. Analyzing single-sweep intensity traces from the FDML laser, a distinct dependence on the tuning frequency can be observed. A dramatically reduced noise can be realized for a narrow range of wavelengths. The reduced noise can be explained by the absence of beating noise due to a fixed phase relation between the laser cavity modes, comparable to standard mode-locked lasers. However, it can be seen that the range of low noise does not cover the entire sweep span, an effect that can be attributed to cavity dispersion and wavelength-dependent birefringence in the cavity. The spectral position of this region is dependent on the tuning frequency of the filter and indicates the region of perfect or near-perfect synchronization between the filter drive and cavity round trip time.

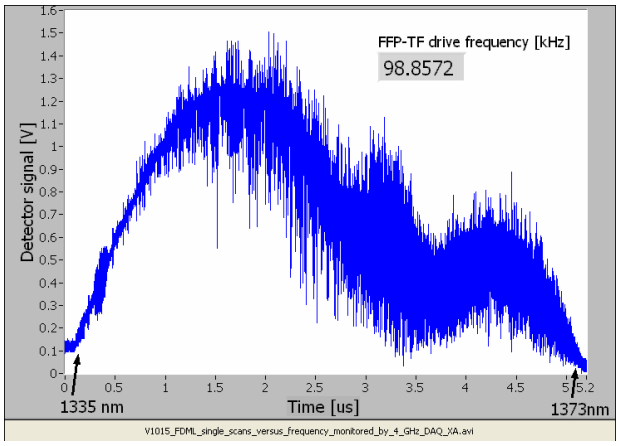

Fig. 2. (One frame of 1.9 MB .avi movie) Individual intensity traces for the FDML laser used in this experiment at different FFP-TF drive frequencies, recorded at high temporal resolution (~ 120 ps). At 120 ps time resolution, the relative beating noise is predicted to increase to 66% RMS [16]. At the lowest FFP-TF drive frequency, the FDML laser is detuned sufficiently that no mode-locking occurs; the high noise is attributed to beating. At slightly higher drive frequencies, patches of low noise appear.

Although we have achieved excellent performance over narrower wavelength spans (~ 5 nm), we have not yet extended this region to the required 38 nm. Narrow wavelength regions of low noise are present, particularly at the highest drive frequencies shown, and these are attributed to narrow regions of perfect or near-perfect mode-locking. The observed dynamics in these spectral regions are not yet fully understood. The increased noise away from these regions is attributed to beating noise. For the present experiments, we chose to operate the laser at the lowest frequency shown in Fig. 2, a frequency of 98,854.5 Hz. Although a higher noise is present throughout the sweep at this drive frequency, a higher stability in the linewidth performance is observed. In the low-noise regions present in the non-detuned case, sweep-to-sweep instabilities in the recorded spectra are observed. These instabilities can be easily seen by viewing live absorption spectra of ambient humidity with the split-pulse reference detection scheme described in Section 3.2. The H_2O absorption features appear to flicker on and off, an artifact which can be understood by a discontinuous tuning behavior of the laser, at times missing or partially missing spectrally narrow absorption features. In

#87089 - $15.00 USD Received 31 Aug 2007; revised 19 Oct 2007; accepted 23 Oct 2007; published 31 Oct 2007

contrast, the features appear significantly more stable in the detuned case. Since stable, high-quality absorption spectra are critical to the thermometry goals of these experiments, we chose to operate the laser in the detuned mode despite the higher intensity noise. This ensures a constant noise level over the entire sweep and provides smooth tuning characteristics. At this frequency, the emission characteristics are comparable to a thermal emitter. An advanced detection system detailed in the next section was applied to compensate for beating noise.

The observed noise characteristic can be explained by the sketch in Fig. 3. The two situations correspond to the cases: (a) The case with a slight detuning of FFP-filter drive frequency and optical roundtrip time in the FDML laser; (b) the case where the FFP-filter drive frequency is well matched to the optical roundtrip time.

In the slightly detuned case (a) there is a constant uncertainty in wavelength at each point in time on a time scale faster than that for one data acquisition point. This corresponds to the model of a narrowband light source (about 0.1 nm in our case) with a monotonically changing center wavelength. All fluctuations in the center wavelength are on a time scale shorter than the acquisition time for one sampling point and the center frequency, as well as the instantaneous linewidth, is approximately constant between different sweeps. If an absorption feature with a linewidth narrower than the instantaneous linewidth of the source is measured, the absorption feature will appear broadened and with lower amplitude, but stable. Case (a) corresponds to the tuning frequency of 98,854.5 Hz in Fig. 2, the slightly detuned case with higher amplitude noise.

In case the frequency matched case (b) the uncertainty in wavelength at each point in time is smaller. The laser has a narrower instantaneous linewidth. However there are discontinuities in the time dependent tuning characteristic. The light source exhibits wavelength jumps, similar to mode hops in classical tunable lasers. However, in the case of FDML lasers, the cavity mode spacing is extremely narrow with values of ~100 kHz, corresponding to 0.5 fm at 1300 nm. Thus, due to the time-frequency uncertainty relation, it is fundamentally impossible to resolve wavelength discontinuities caused by classical laser mode hops during a sampling gate time of about 10 ns. As a consequence, the observed wavelength jumps are related to other mechanisms or caused by sub-cavity structures within the laser. The discontinuities exhibit a poor sweep to sweep stability and may occur at different points in time during one cycle. This model is supported by the observation of narrowband H_2O absorption features flickering on and off. This observation is in agreement with a very narrowband instantaneous linewidth (about 10 pm) tuning with discontinuities that are non-reproducible in time. For any sweep in which the source exhibits such a wavelength jump in the region of a certain H_2O absorption line, the line cannot be seen.

In both cases, the instantaneous linewidth as well as the tuning discontinuities represent an uncertainty in wavelength. The difference between them is the time scale on which they occur. The term “instantaneous linewidth” is commonly applied for wavelength uncertainty caused by drift and jitter on a time scale much faster than the sampling or measurement time, in our case faster than 10 ns. The term wavelength jitter is used for wavelength uncertainty on a time scale slower than the sampling time caused by wavelength jumps and sweep-to-sweep wavelength changes. This model should only be considered as an intuitive picture of the laser output. The real operation and the physical mechanisms behind it are not yet well understood. Because it is difficult to build real time spectrometers with an acquisition rate of several 100 MHz and a resolution of several pm over a 100 nm range, the temporal evolution of the instantaneous laser linewidth can only be measured indirectly.

#87089 - $15.00 USD Received 31 Aug 2007; revised 19 Oct 2007; accepted 23 Oct 2007; published 31 Oct 2007

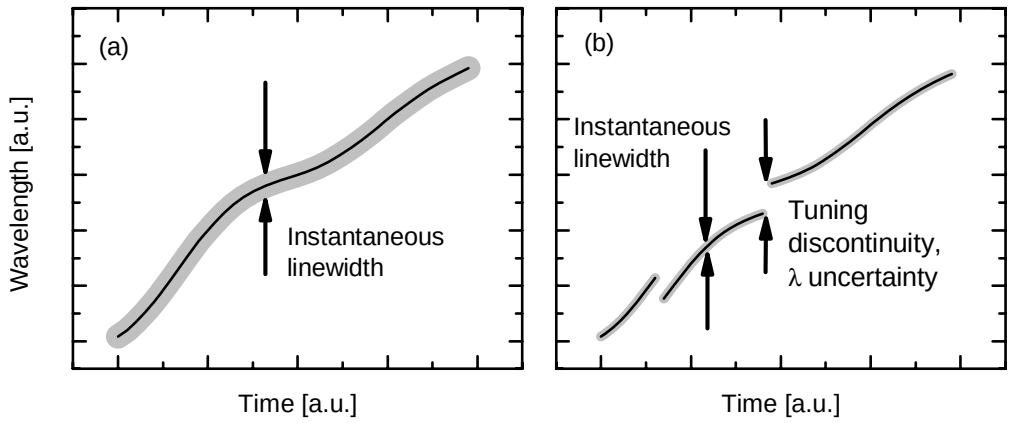

Fig. 3. Two cases of wavelength swept laser operation. (a) Drive frequency of FFP-filter in the FDML laser and optical roundtrip time slightly detuned. (b) Drive frequency and roundtrip time well matched.

3.2 Split pulse data acquisition for noise suppression using optical time multiplexing

A unique experimental configuration was implemented to eliminate beating noise originating from the FDML laser. The approach is roughly patterned after common referencing strategies based on multiple detectors [6] or on a single dual-balanced detector [5]. One complication with the latter approach is that the dual-balanced detector is designed to provide the difference rather than the ratio of two signals; while the ratio is generally needed for direct absorption spectroscopy. Furthermore, in both of these common referencing strategies, one often relies on perfect matching of two photodiodes, and this is especially difficult when significant signal content is present near the bandwidth limit of the system. To circumvent these challenges, the present referencing strategy uses only a single detector and the signal is optically multiplexed in time.

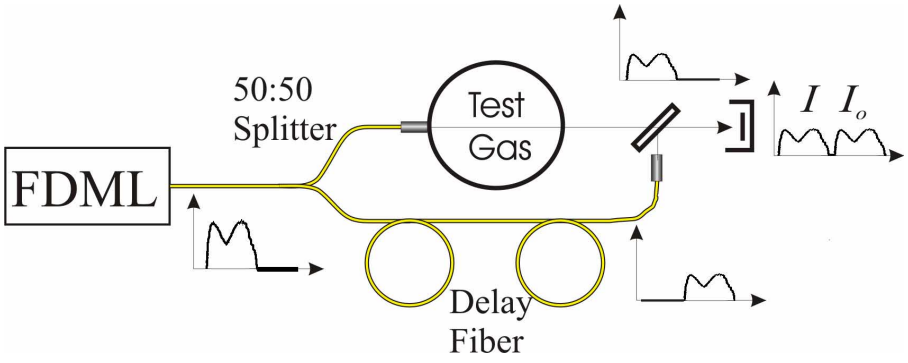

Fig. 4. Experimental configuration for reducing the minimum detectable absorbance in the presence of beating noise. Half of the light is directed through the engine, and half through a delay fiber. The light is recombined with a free-space beam splitter and the two signals are measured consecutively using a single photoreceiver.

The FDML source was operated at 50% duty cycle (on for the 5 μs that the laser swept from 1335 nm to 1373 nm, and off for the 5 μs that the laser would be sweeping from 1373 nm to 1335 nm). The 5 μs scan was split by a 50:50 coupler; one leg was directed immediately through the engine, and the other leg was delayed 5 μs using a ~1000 m length of

#87089 - $15.00 USD Received 31 Aug 2007; revised 19 Oct 2007; accepted 23 Oct 2007; published 31 Oct 2007

fiber. The two paths were then re-combined at the photoreceiver using a free-space beam splitter, as show in Fig. 4. Imperfect wavelength-flatness in the 50:50 coupler can be a limitation insofar as it compromises the signal-to-noise-ratio of the final result by requiring increased dynamic range in the detection. Chromatic dispersion in the delay line can also introduce artifacts, but was not a limitation here, in part because a low-dispersion fiber (Fujikura USS) was used. Polarization paddles were used both within the laser cavity, and at the end of the delay fiber. By monitoring absorbance rather than raw signal, the paddles could be adjusted to minimize noise in the final absorbance spectra.

3.3 Design of the optical engine

Experiments were performed in a single-cylinder research engine adapted for optical access. Relevant engine details including drawings, intake system arrangement, and cylinder pressure instrumentation have been published previously [19]; a brief description is also provided here. The engine has an 11:1 compression ratio, a bore of 86 mm, and a stroke of 94.6 mm, resulting in a displaced volume of 550 cm^3. The cylinder head features a pent-roof geometry with two intake and two exhaust valves actuated with fixed overhead cams.

Line-of-sight optical access to the combustion chamber was achieved through windows mounted in two pressure transducer ports machined into opposite sides of the combustion chamber, in line with the pent-roof. Diagrams showing the beam location are provided in Fig. 5. The windows used were sapphire rods: 47.5 mm long x 2.8 mm diameter with a clear aperture of ~1 mm for the input window, and 50.8 mm long x 4.6 mm diameter with a clear aperture of ~2 mm on the output window. The clear apertures are set by the original design of the pressure transducer ports that were machined into the engine head. In future tests, we plan to use windows made of an amorphous material such as fused silica, because the sapphire rod windows caused a periodic modulation in the wavelength scan transmitted through the engine. The modulation was attributed to a birefringence associated with the crystal structure of sapphire and its orientation in these windows. For the present experiments, the modulation was eliminated by inserting a free-space polarizer at the input to the engine and tuning the rotation of the sapphire windows about the laser beam axis.

Cylinder pressure was measured using a Kistler 6125B piezoelectric pressure transducer coupled with a Kistler 5010B dual mode charge amplifier. Because the original pressure transducer ports were used for optical access in the pent roof, the pressure transducer was mounted into an adapter fitted to spark plug hole of the cylinder head. The cylinder pressure data were low-pass filtered at 8 kHz and recorded at half-crank angle increments. Acquisition triggering was provided by an optical shaft encoder (BEI model H25). The engine control unit (ECU) was used to provide a one-per-cycle trigger to synchronize the optical measurements to the engine cycle.

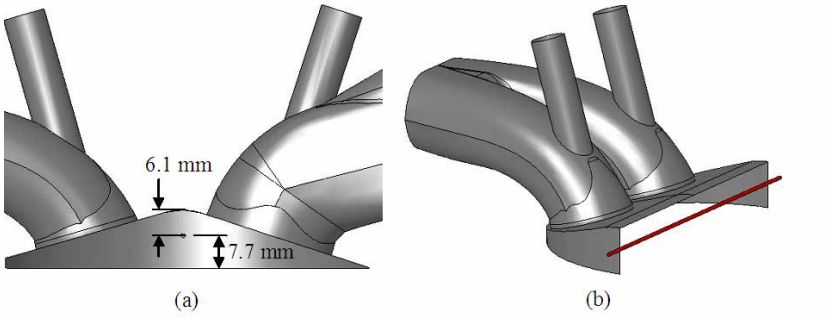

Fig. 5. Side (a) and isometric (b) views detailing the laser beam path through the combustion chamber. The laser beam is located 6.1 mm from the peak of the pent-roof and 7.7 mm from the fire deck, which for the present engine corresponds to the top of the piston at top dead center.

#87089 - $15.00 USD Received 31 Aug 2007; revised 19 Oct 2007; accepted 23 Oct 2007; published 31 Oct 2007

Airflow to the engine was metered using a calibrated critical flow orifice and was adjusted to maintain an atmospheric intake manifold pressure. The intake air was heated using resistance heaters wrapped around the tanks of the intake system. The heaters were controlled using thermocouple temperature measurements made throughout the intake system. The last temperature measurement prior to induction into the engine was made ~10 cm upstream of the intake valves.

Water vapor was seeded into the engine so that temperature could be calculated while the engine motored on otherwise dry intake air. This was accomplished using a pressure cooker attached with a heated, insulated stainless steel pipe plumbed to the air intake. The pressure cooker elevated the pressure of H_2O vapor to approximately 2 bar. A pin valve allowed fine adjustment of the mass flow of the vapor entering the air intake. In firing engine studies, water vapor seeding is not usually necessary, since there is sufficient water produced during combustion and recirculated into subsequent engine cycles.

4. Results

Each scan of the laser was converted into an absorbance spectrum using Beer's Law, and temperature was inferred using a previously described recipe [20]. Except where noted, adjacent spectra within a single crank angle degree (CAD) were averaged (a total of 28 sequential spectra at 600 rpm), as shown in the red trace of Fig. 6.

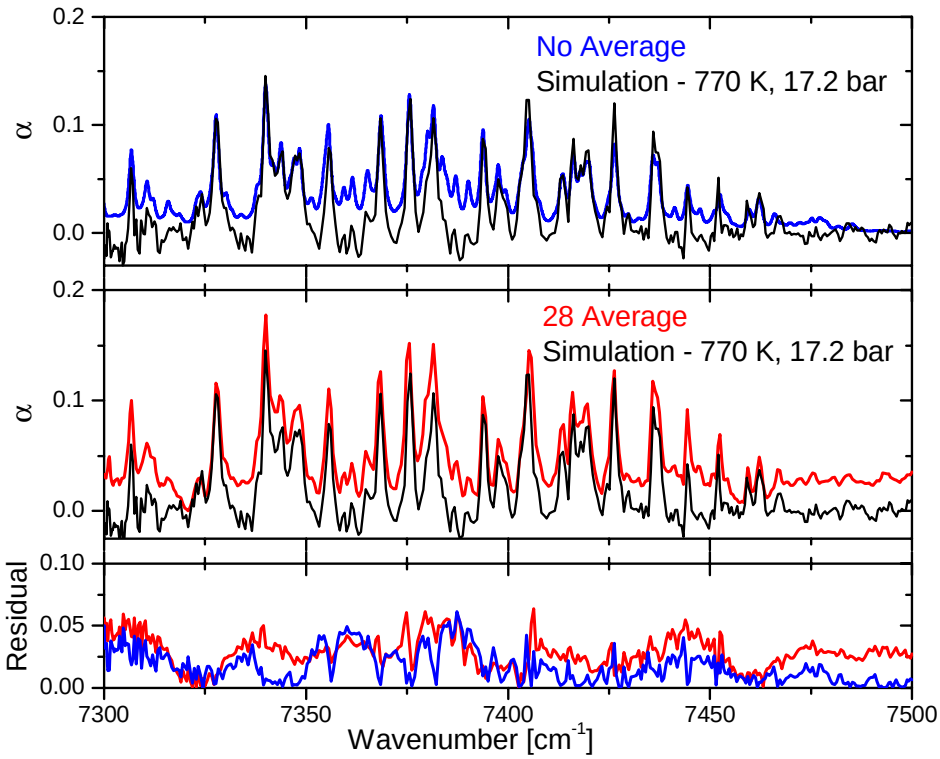

Fig. 6. *Upper panel*: Absorbance (base e) spectrum measured at top dead center (TDC) of an engine motoring at 600 rpm (blue). A spectrum simulated from the BT2 database is shown as a reference (black); the conditions of the simulation are based on the best fit of the measured spectrum. *Middle panel*: Average of 28 sequential measured spectra (corresponding to 1 CAD) around TDC (red) with reference simulated spectrum (black). *Lower panel*: RMS difference between measured and simulated spectra (blue = no average, red = 28 average).

#87089 - $15.00 USD Received 31 Aug 2007; revised 19 Oct 2007; accepted 23 Oct 2007; published 31 Oct 2007

Non-averaged spectra individually exhibited 1-2% peak-to-peak noise (blue trace of Fig. 6). Note that this noise level is similar to that previously obtained [5] by averaging 50 spectra together. The lower panel of Fig. 6 shows that the RMS residual between the measured and simulated spectra are similar for the single and averaged spectra. The improvement in noise is attributed to the use of the split-pulse detection scheme versus a dual-balanced detector (Thorlabs PDB-150C) and from the use of a 14-bit oscilloscope versus an 8-bit oscilloscope. The measurements shown in Fig. 6 represent absorbance spectra measured at top dead center (TDC) in the engine motoring at 600 rpm; the red trace is the average from -0.5 to +0.5 CAD. The best-fit simulated H_2O spectrum (black) is based on the pressure measured by the cylinder transducer (17.4 bar), temperature inferred from the red trace (770 K) using [20], with line strengths, positions, and lower-state energies taken from the BT2 line list [21] and line-broadening approximated using the correlation in [20]. Both measured traces in Fig. 6 have a spline-fit baseline added for clarity of presentation; however, the baseline fit is not used for calculating temperature. The temperature calculation involves a differentiation step which automatically eliminates baseline drifts [20]. The accuracy of the measured temperatures ultimately depends upon the accuracy of the BT2 line list. Based on preliminary simulations, we estimate the accuracy of temperatures measured using the described approach to be better than 1% up to at least 2000 K. Controlled experiments are underway to validate this expectation.

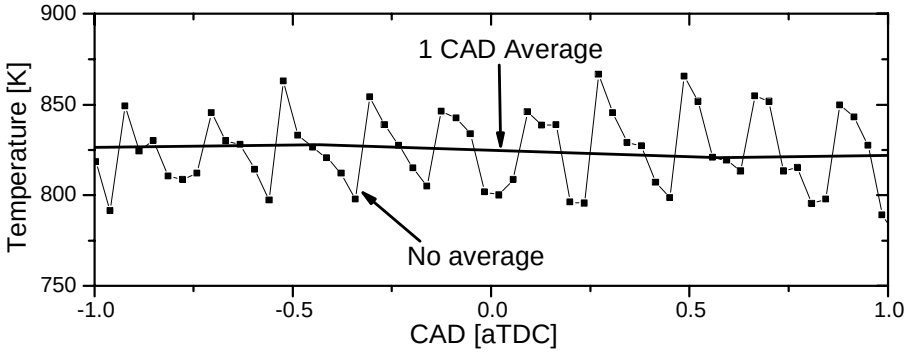

Fig. 7. Temperature calculated from water absorption spectra as a function of crank angle, each point representing 10 μs of recorded data. This plot highlights the repeatable pattern attributed to trigger jitter.

Despite the low noise in individual spectra, calculated single-shot temperatures were plagued by problems associated with a trigger jitter, as seen in Fig. 7. There is at least one sample of jitter associated with the triggering. At the sample rate of 100 MHz (10 ns per sample), this corresponds to a jitter of ~0.1 nm in the wavelength axis. As temperatures inferred from molecular spectra are sensitive to the accuracy of the wavelength axis, this jitter accompanies the temperature jitter seen in Fig. 7. Improved, higher-bandwidth triggering on the 400 MS/s oscilloscope planned for future tests is expected to eliminate this jitter and dramatically improve the precision of the single-scan data.

#87089 - $15.00 USD Received 31 Aug 2007; revised 19 Oct 2007; accepted 23 Oct 2007; published 31 Oct 2007

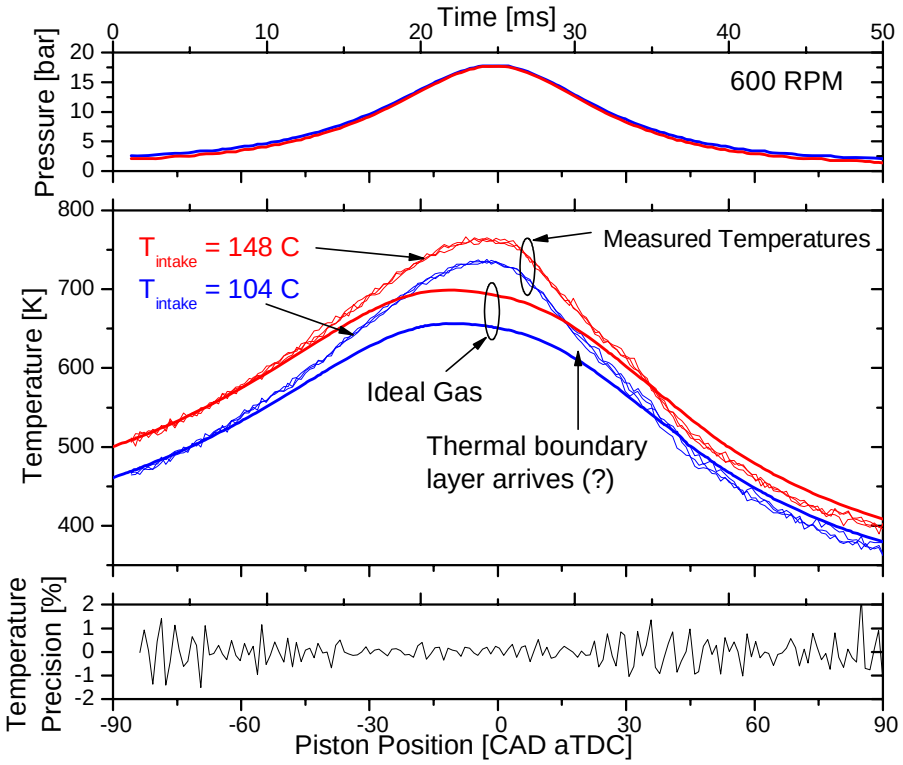

Fig. 8. Ideal gas temperature calculations (thick lines) and temperature calculated from absorption spectra (1 CAD average) versus crank angle degrees (CAD) from a motoring engine running at 600 rpm. The engine cycles had the intake air heated to 104 °C (blue), and 148 °C (red). Each measured point is calculated from H_2O spectra averaged over 1 CAD. The measured temperatures for 3 consecutive engine cycles are shown in each case.

Fig. 8 shows the calculated temperatures versus crank angle degrees (CAD) from 90 CAD before top dead center (TDC) to 90 CAD after TDC for an engine motoring at 600 rpm. Two conditions were measured, one in which the air intake temperature was 104 °C, and one in which it was 148 °C. Ideal gas temperature estimations based on pressure transducer and overall mass flow measurements for the two conditions are shown using thick lines. The results of three engine cycles for each of the two conditions are shown using thinner lines. A large amount of blow-by is expected in this engine modified for optical probing. The blow-by can be observed by noting that the actual measured temperature becomes hotter than the ideal gas temperature prediction with higher pressures. Some of this discrepancy can also be attributed to heat transfer effects not included in the ideal-gas-law estimation. The bottom panel of Fig. 8 shows the temperature precision calculated from one of the T_{intake} = 104 °C (blue) traces. The precision is calculated as the percent deviation of the trace from a smoothed (10-CAD-adjacent-averaged) version of the same trace. The less-precise results at early crank-angles (before -35 CAD) are attributed to lower in-cylinder pressure which ultimately causes reduced signal-to-noise ratio in the absorption spectra because of instrumental broadening. On the expansion stroke, the situation is more complicated.

#87089 - $15.00 USD Received 31 Aug 2007; revised 19 Oct 2007; accepted 23 Oct 2007; published 31 Oct 2007

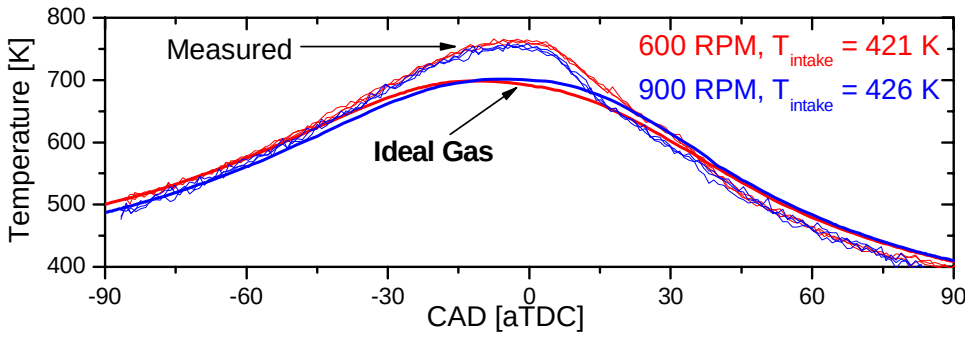

Fig. 9. Ideal gas temperature calculations and temperature calculated from absorption spectra versus crank angle degrees (CAD) from a motoring engine running at 600 rpm (red) and 900 rpm (blue). Each measured point is calculated from H_2O spectra averaged over 1 CAD. Again the measured data correspond to three consecutive engine cycles.

The same effect of increased noise at reduced pressures is expected; however this should occur at roughly +30 CAD because the pressure trace is roughly symmetric. Instead, precision effects (and even more dramatically, cycle-to-cycle deviations directly visible in the middle panel of Fig. 8) begin near +20 CAD. We believe that the dominant effect during the expansion stroke is a thermal boundary layer that grows from the engine head surface down into the beam path. This thermal boundary layer contains colder gas with a higher degree of inhomogeneity than the in-cylinder gas at earlier crank angles. Presumably, the inhomogeneities are different from cycle-to-cycle, leading to the deviations that can be seen in the middle panel of Fig. 8. Ultimately, this colder gas causes the measured temperatures to drop below the ideal-gas-law temperatures because the latter considers the entire cylinder volume while the former samples only the colder boundary layer.

Fig. 9 shows the results for similar engine conditions run at 600 rpm (red) and 900 rpm (blue). Note that less blow-by and heat transfer is observed in the 900 rpm case; this is expected, since there is less time for these effects to act.

4. Conclusion and outlook

A Fourier-domain mode-locked (FDML) laser has been developed for piston engine gas thermometry. The center wavelength was designed to be ~1350 nm to coincide with a temperature-sensitive region of H_2O absorption, and the laser was modulated with a 50% duty cycle to allow a split-pulse referencing scheme appropriate for absorption spectroscopy. It is interesting to note that a single FDML laser could be used to simultaneously acquire depth resolved, tomographic scattering information such as in optical coherence tomography *and* engine temperature traces, if desired.

Crank-angle-resolved gas temperatures were measured in an engine motoring at 600 and 900 rpm with a precision of ~1%. The engine was not fired in this study because of concerns associated with engine safety (the engine includes a quartz ring, not used in these experiments, that was designed primarily for motoring measurements). Nonetheless, hot combustion gases can be monitored readily by this sensor and in fact have been done successfully in a cycle-averaged mode [5] before the low-noise (split-pulse-referenced) approach described here was adopted.

Improvements compared with previous studies [5], came from two main techniques introduced in this paper. The stability of the laser was improved by detuning the frequency of the filter with the round trip time of the light. This minimized irregular tuning discontinuities. Also, the split-pulse strategy was introduced as a way to minimize collecting noise originating from the laser.

The absolute accuracy of the measurements depends almost entirely on the fidelity of the BT2 database. The temperature results obtained using the full-spectral least-squares matching

#87089 - $15.00 USD Received 31 Aug 2007; revised 19 Oct 2007; accepted 23 Oct 2007; published 31 Oct 2007

to BT2 as described here are expected to have an absolute accuracy of better than 1% up to 2000 K based on theoretical arguments, but controlled experiments are underway to confirm this expectation. Some averaging of adjacent laser sweeps was used in these experiments to reach the 1% precision level, and was allowed by the crank-angle resolution requirement (1 CAD ~ 280 μs or 28 adjacent laser scans at 600 rpm). However, the primary effect of this averaging was to smooth trigger jitter effects that can be reduced directly using a higher-speed data acquisition system (we are currently in the process of upgrading from 100 MS/s to 400 MS/s). By reducing the trigger jitter, we are confident that thermometry with ~1% precision can be performed without any averaging of adjacent laser sweeps. This capability will enable this optical thermometer to become new optical tool for measurements in highly dynamic events such as detonations and explosions.

Acknowledgments

This research is supported by the Air Force Office of Scientific Research and Medical Free Electron Laser Program FA9550-040-1-0046 and FA9550-040-1-0011, National Science Foundation ECS-0501478, BES-0522845, and CTS-0238633, and the Department of Energy FreedomCAR and Vehicle Technologies University Project# DE-FC26-06NT42628. R. Huber is supported by the Emmy Noether program of the German Research Foundation (DFG) HU1006/2-1.

#87089 - $15.00 USD Received 31 Aug 2007; revised 19 Oct 2007; accepted 23 Oct 2007; published 31 Oct 2007